

SUPPLEMENTARY MATERIAL TO

PITX2 deficiency leads to atrial mitochondrial dysfunction

Jasmeet S. Reyat ^{1,2*,#}, Laura C. Sommerfeld ^{1,3,4,5 *}, Molly O'Reilly ¹, Victor R. Cardoso ^{1,6}, Ellen Thiemann ^{3,4,7}, Abdullah O. Khan¹, Christopher O'Shea ¹, Sönke Harder ⁸, Christian Müller ⁹, Jonathan Barlow¹⁰, Rachel J. Stapley ¹, Winnie Chua ¹, S. Nashitha Kabir ¹, Olivia Grech ¹, Oliver Hummel ¹¹, Norbert Hübner ^{12,13}, Stefan Kääb ^{14,15}, Lluís Mont ^{16,17}, Stéphane N. Hatem ¹⁸, Joris Winters ¹⁹, Stef Zeemering ¹⁹, Neil V. Morgan ¹, Julie Rayes ¹, Katja Gehmlich ¹, Monika Stoll ^{20,21}, Theresa Brand ²², Michaela Schweizer ²³, Angelika Piasecki ⁷, Ulrich Schotten ¹⁹, Georgios V. Gkoutos ⁶, Kristina Lorenz ^{22,24}, Friederike Cuello ^{4,7}, Paulus Kirchhof ^{1,3,4 #} and Larissa Fabritz ^{1,3,4,5}

¹ Institute of Cardiovascular Sciences, College of Medical and Dental Sciences, University of Birmingham, Wolfson Drive, Birmingham, UK

² Division of Cardiovascular Medicine, Radcliffe Department of Medicine, University of Oxford, John Radcliffe Hospital, Oxford, UK

² Department of Cardiology, University Heart and Vascular Center Hamburg, University Medical Center Hamburg-Eppendorf, Martinistraße 52, 20246 Hamburg, Germany

³ DZHK (German Center for Cardiovascular Research), partner site Hamburg/Kiel/Lübeck, University Medical Center Hamburg-Eppendorf, Germany.

⁴ University Center of Cardiovascular Sciences, University Medical Center Hamburg-Eppendorf, Germany

⁵ Institute of Cancer Genomics, College of Medical and Dental Sciences, University of Birmingham, Birmingham, UK

⁶ Institute of Experimental Pharmacology and Toxicology, Cardiovascular Research Center, University Medical Center Hamburg-Eppendorf, Martinistrasse 52, 20246 Hamburg, Germany.

⁷ Institut für Klinische Chemie und Laboratoriumsmedizin, Massenspektrometrische Proteomanalytik, University Medical Center Hamburg-Eppendorf, Martinistrasse 52, 20246 Hamburg, Germany

⁸ UKE Bioinformatics Core; University Medical Center Hamburg-Eppendorf, Martinistrasse 52, 20246 Hamburg, Germany

⁹ Cellular Health and Metabolism Facility, College of Life and Environmental Sciences, University of Birmingham, Birmingham, UK

¹⁰ Max Delbrück Centrum for Molecular Medicine, Berlin, Germany, Charité - Universitätsmedizin Berlin, German, and German Center for Cardiovascular Research (DZHK), partner site Berlin

¹¹ Charité - Universitätsmedizin Berlin, Germany

¹² German Center for Cardiovascular Research (DZHK), Partner Site Berlin, Germany

¹³ Department of Medicine I, University Hospital Munich, Ludwig Maximilian University of Munich (LMU), Munich, Germany

¹⁴ German Centre for Cardiovascular Research (DZHK), partner site Munich Heart Alliance, Munich, Germany

¹⁵ Hospital Clínic, Universitat de Barcelona, Catalonia, Spain
and Institut de Recerca Biomèdica, August Pi- i Sunyer, Barcelona, Catalonia, Spain

¹⁶ Centro Investigación Biomédica en Red Cardiovascular, Madrid, Spain

¹⁷ INSERM UMRS1166, ICAN - Institute of Cardiometabolism and Nutrition, Sorbonne University, Institute of Cardiology, Pitié-Salpêtrière Hospital, Paris, France

¹⁸ Cardiovascular Research Institute Maastricht, Department of Physiology, Maastricht University, Maastricht, The Netherlands

¹⁹ Institute of Human Genetics, Genetic Epidemiology, WWU Münster, Germany

²⁰ Cardiovascular Research Institute Maastricht, Genetic Epidemiology and Statistical Genetics, Maastricht University, Maastricht, Netherlands

²¹ Institute of Pharmacology and Toxicology, University of Würzburg, Würzburg, Germany

²² Department of Morphology and Electron Microscopy, Center for Molecular Neurobiology, University Medical Center Hamburg-Eppendorf, 20246, Hamburg, Germany

²³ Leibniz-Institut für Analytische Wissenschaften – ISAS – e.V., Dortmund, Germany

***Co-first Authors**

#Corresponding Authors:

Paulus Kirchhof
Department of Cardiology
University Heart and Vascular Center Hamburg
University Medical Center Hamburg-Eppendorf
Martinistrasse 52
20246 Hamburg
Germany
p.kirchhof@uke.de
+49 40 741053824 (Judith Ebeling)

Jasmeet S. Reyat
Department of Cardiovascular Medicine
Radcliffe Department of Medicine
University of Oxford
John Radcliffe Hospital
Oxford
UK
jasmeet.reyat@cardiov.ox.ac.uk
+44 (0)186 523 4915

Author ORCID IDs:

JSR – 0000-0003-3247-9186
LCS – 0000-0001-9837-8770
MOR – 0000-0003-1936-5838
VRC – 0000-0002-9588-6304
AOK – 0000-0003-0825-3179
COS – 0000-0003-3030-7364
SH – 0000-0002-6352-4771
JB – 0000-0002-9463-7234
RJS – 0000-0002-0027-9158
WC – 0000-0002-6747-8813
SNK – 0000-0003-1811-8683
OG – 0000-0001-5560-802X
OH – 0009-0000-9986-8333
NH – 0000-0002-1218-6223
TB – 0000-0002-0630-4537
MS – 0000-0001-5062-328X
LM – 0000-0002-8115-5906
JW – 0000-0002-4945-3946
SZ – 0000-0003-3738-7328
NVM – 0000-0001-6433-5692
JR – 0000-0003-0499-6880
KG – 0000-0003-4019-1844
FC – 0000-0003-1612-1715
MSt – 0000-0002-2711-4281
KL – 0000-0002-5747-2207
US – 0000-0003-1532-3315
GVG – 0000-0002-2061-091X
PK – 0000-0002-1881-0197
LF- 0000-0002-9241-1733

Supplementary Materials and Methods:

Generation of *PITX2* KO human induced-pluripotent stem cells (hiPSCs)

PITX2 knockout (KO) hiPSCs were generated based on a previously described protocol (1). Briefly, human fetal fibroblasts were transfected with a self-replicating RNA vector expressing four reprogramming factors to generate integration-free wild-type hiPSCs. Following antibiotic selection to maintain transgene expression, the F1 hiPSC line was maintained under normal culture conditions and displayed typical hiPSC morphology and karyotype (1). Validation of the F1 hiPSC line to differentiate into all three germ layers has previously been described (1).

The *PITX2* gene is made up of 7 exons and gives rise to three different isoforms (*PITX2a*, *PITX2b* and *PITX2c*) that are generated through alternative splicing and differential promoter activation. Two CRISPR/Cas9 nickase vectors were designed to target the 5' end of exon 6 which is expressed by all *PITX2* isoforms, to potentially induce frame shift-causing deletion mutations in a controlled manner (Supplementary Figure 1A). Genomic sequencing of both *PITX2* clones revealed a 58 base-pair deletion in the *PITX2* KO1 line and a 60 base-pair deletion in the *PITX2* KO2 line followed by frame-shift causing deletions leading to a premature stop codon (Supplementary Figure 1A). Pluripotency of the two *PITX2* KO lines was characterized using microscopy and flow cytometry staining. Both *PITX2* KO lines and the parental WT line displayed characteristic human embryonic stem cell morphology. Flow cytometry staining for the pluripotency markers OCT4 and SOX2 showed that both *PITX2* KO and WT hiPSCs showed >98% dual-positive staining (Supplementary Figure 1C). These results confirm the successful generation of a hiPSC line that contains a homozygous deletion of *PITX2*.

Bulk RNA-Sequencing sample processing of human left atrial appendages

Total RNA was extracted from the atrial biopsies using the Direct-zol RNA MiniPrep Plus Kit (Zymo Research, R2073), including an in-column DNase I treatment. RNA was initially quantified with a NanoDrop 8000 UV-Vis Spectrophotometer (Thermo Scientific) and quality was assessed using the Bioanalyzer RNA 6000 Nano Kit (Agilent). Samples with sufficient quantity and quality (RNA integrity number ≥ 6) were retained for sequencing. The NEBNext Poly(A) mRNA Magnetic Isolation Module (New England Biolabs, E7490) was then used to select poly-A tailed (largely messenger RNA) molecules from total RNA. The purified mRNA was used to prepare a directional cDNA library for sequencing using the NEBNext Ultra Directional RNA Library Prep Kit for Illumina (New England Biolabs, E7420L). Quality control (before and after library preparation) was done using the Bioanalyzer HighSens DNA Kit (Agilent, 5067-4626) and the molarity was checked using the Kapa qPCR quantification kit (Roche Diagnostics, KK4824). Paired-end, 80 base pair sequence was generated using an Illumina NextSeq500, with the version 2 chemistry. After de-multiplexing and adapter removal, per sample sequence quality was assessed with FastQC.

Karyotyping

hiPSCs were incubated for 3 hours in Gibco StemFlex Medium with 50 ng/ml Colcemid (Thermo Fisher Scientific, 152120-012). The cells were collected and treated with 0.075 M KCl for 30 minutes

at 37°C and then treated with methanol:acetic acid (3:1) for a further 20 minutes at room temperature to fix the cells. The chromosome suspension was dropped onto glass slides, air-dried, and stained with 4',6-diamidino-2-phenylindole (DAPI) in ProLong Gold Antifade reagent (Thermo Fisher Scientific, P36931). A minimum of 25 metaphase images were acquired for all the hiPSC lines and the chromosome number was counted for all the metaphase spreads using a Leica TCS SPE confocal microscope (Leica Microsystems).

Proteomics sample preparation and analysis

Tryptic digestion

Atrial cardiomyocytes were dissolved in 100 mM triethyl ammonium bicarbonate and 1% w/v sodium deoxycholate buffer, boiled at 95 °C for 5 min and sonicated with a probe sonicator. Disulphide bonds were reduced with (1 µL, 1M dithiothreitol for 30 min, alkylated in the presence of (4 µL, 0.5 M) iodoacetamide for 30 min in the dark and digested with (1.5 µL trypsin 1µg/µL (sequencing grade, Promega) at 37 °C overnight. SDC was precipitated by the addition of 1% v/v formic acid followed by centrifugation at 16,000 g and the supernatant was transferred into a new tube. Samples were dried in a vacuum centrifuge. For LC-MS/MS analysis, samples were dissolved in 20 µL 0.1% FA

LC-MS/MS analysis

Protein identification via analysis of the tryptic peptides by LC-MS/MS was achieved by injection of the samples onto a nano-liquid chromatography system (Dionex UltiMate 3000 RSLCnano, Thermo Scientific) coupled via electrospray-ionization (ESI) to a mass spectrometer (MS) equipped with a quadrupole, a linear trap and an orbitrap (Orbitrap Fusion, Thermo Scientific). The samples were injected (5 µL/min) to a trapping column (Acclaim PepMap µ-precolumn, C18, 300 µm x 5mm, 5 µm, 100 Å, Thermo Scientific; buffer A: 0.1% FA in HPLC-H₂O; buffer B: 0.1% FA in ACN) with 2% buffer B. After sample injection the trapping column was washed for 5 min with 2% buffer B (5 µL/min). Peptides were moved to (200 nL/min) the separation column and separated on this column (Acclaim PepMap 100, C18, 75 µm x 250 mm, 2 µm, 100 Å, Thermo Scientific; 200 nL/min, gradient: 2–30% B in 30 min). The spray was formed by a fused-silica emitter (I.D. 10 µm, New Objective, Woburn, USA) at a capillary voltage of 1800 V. Mass spectra were measured in the positive ion mode. LC-MS/MS analysis with the orbitrap Fusion were carried out in data dependent acquisition mode (DDA) applying top speed mode. HCD collision energy of 28%, an intensity threshold of 2e5 and an isolation width of 1.6 m/z was used. A MS scan was performed every second over a m/z range from 400–1200 (resolution of 120000 FWHM at m/z 200; transient length= 256 ms; maximum injection time= 50 ms; AGC target= 2e5). MS/MS spectra were obtained in the ion trap (scan-rate= 66 kDa/s; maximum injection time= 200 ms; AGC target= 1e4; underfill ratio of 10%; isolation width of 2 m/z).

Data analysis

With Proteome Discoverer 2.4.1.15 (Thermo Scientific) the LC-MS/MS data were processed. Identification and quantification of the proteins from the MS/MS spectra were performed with the search engine Sequest HT using the homo sapiens SwissProt database (www.uniprot.org). For the searches the following parameters were applied: Precursor mass tolerance: 10 ppm; Fragment mass

tolerance: 0.6 Da. Two missed cleavages were allowed. Carbamidomethylation on cysteine residues as a fixed modification and oxidation of methionine residues as a variable modification was used for the search. Peptides with an FDR of 1% using Percolator were identified. At least two unique peptides per protein were used as a condition for a reliable identification.

The R/Bioconductor package DEP (2) was used for pre-processing and data analysis of protein abundances. Only proteins with maximal three missing values in one condition were included, leading to 3128 proteins used in the analysis. After log2-transformation and variance stabilizing normalization, a k-nearest neighbour approach was used for the imputation of missing values. Differential protein expression was tested using the *test_diff* method from DEP which applies protein-wise linear models and empirical Bayes statistics based on R/Bioconductor package *limma*. False-discovery rates (FDR) were calculated based on the Benjamini-Hochberg method to account for multiple testing. Proteins with an $FDR \leq 0.05$ and an absolute log2-fold-change ≥ 1 were considered significant. The GSEA function from the R/Bioconductor *ClusterProfiler* package (3) was used for gene set enrichment analysis and enriched categories with a $FDR \leq 0.05$ were considered significant.

Whole-cell patch clamp analysis

Membrane potential was defined as the lowest diastolic potential. The measured liquid junction potential (LJP) was +15 mV and membrane measurements were corrected for the LJP offline. Action potential amplitude (APA) was defined as difference between the diastolic membrane potential and the peak potential and was not measured in 1 Hz or 2 Hz stimulated aCMs due to the effect of current injection. Action potential duration (APD) was measured from time of maximum upstroke velocity (dV/dt_{max}) to 30%, 50%, 70% and 90% repolarization (APD30, APD50, APD70 and APD90 respectively).

Automated clustering of action potentials with similar morphologies was achieved using the spectral clustering approach of (4). Processed action potentials used for analysis of action potential parameters (see above) were aligned by time of maximum upstroke velocity, and time windowed 80 ms before and 120 ms after this time. The affinity ($A(i,j)$) between two aligned action potential (AP_i and AP_j) was calculated as

$$A(i,j) = \exp\left(\frac{-d^2(AP_i, AP_j)}{\sigma^2}\right) \quad (1)$$

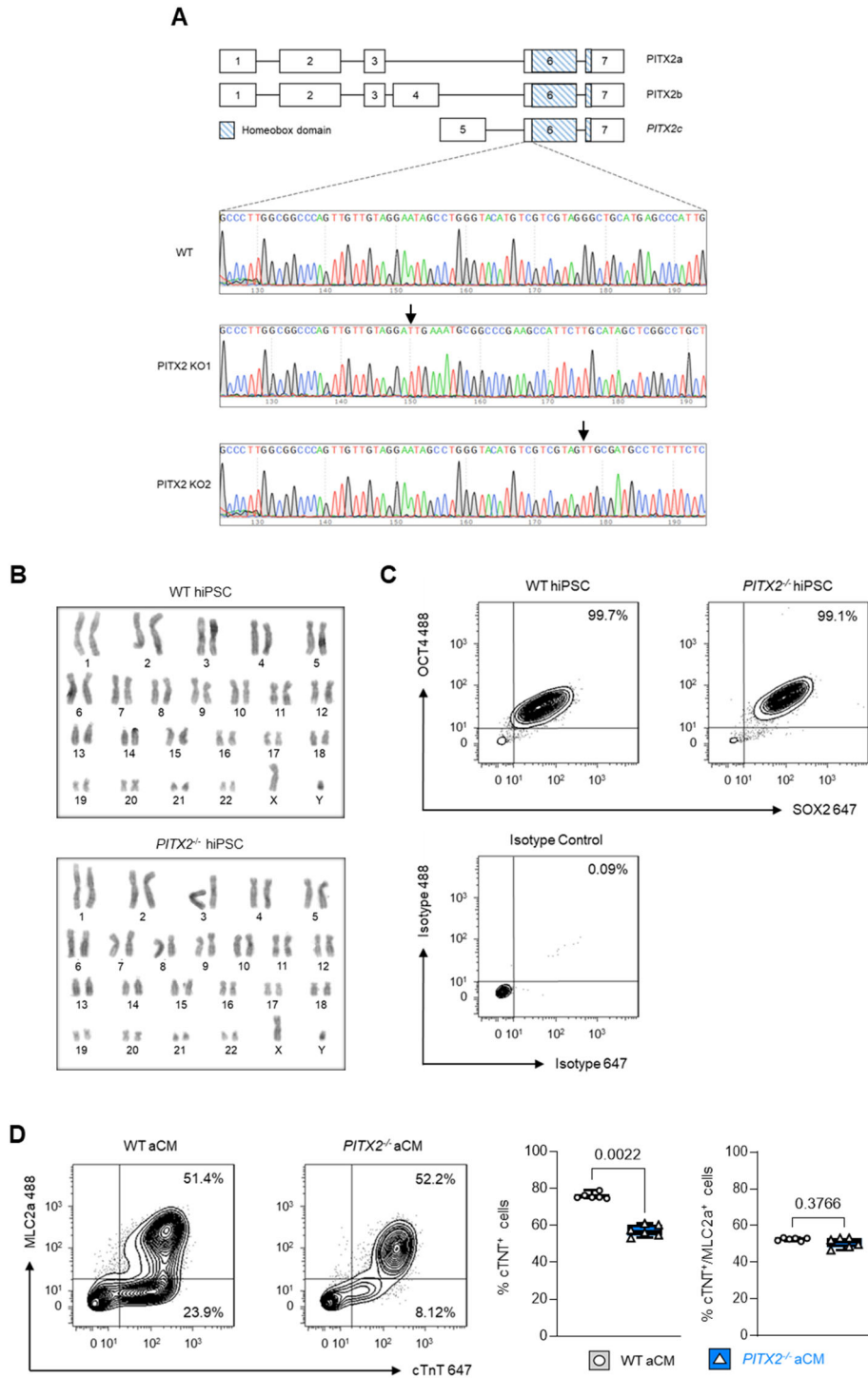
where d is the Euclidean distance between AP_i and AP_j . σ^2 is a scaling parameter and was set as

$$\sigma^2 = \frac{1}{N^2} \sum_{i=1}^N \sum_{j=1}^N d^2(AP_i, AP_j) \quad (2)$$

where N is the number of cells/action potentials (5). This formulation results in affinity, A , approaching 1 when two action potentials have similar morphology, and approaching 0 when action potentials are morphologically distinct. Affinity was calculated for each action potential compared to all other action potentials across the 2 experimental groups. The affinity metric was then used to

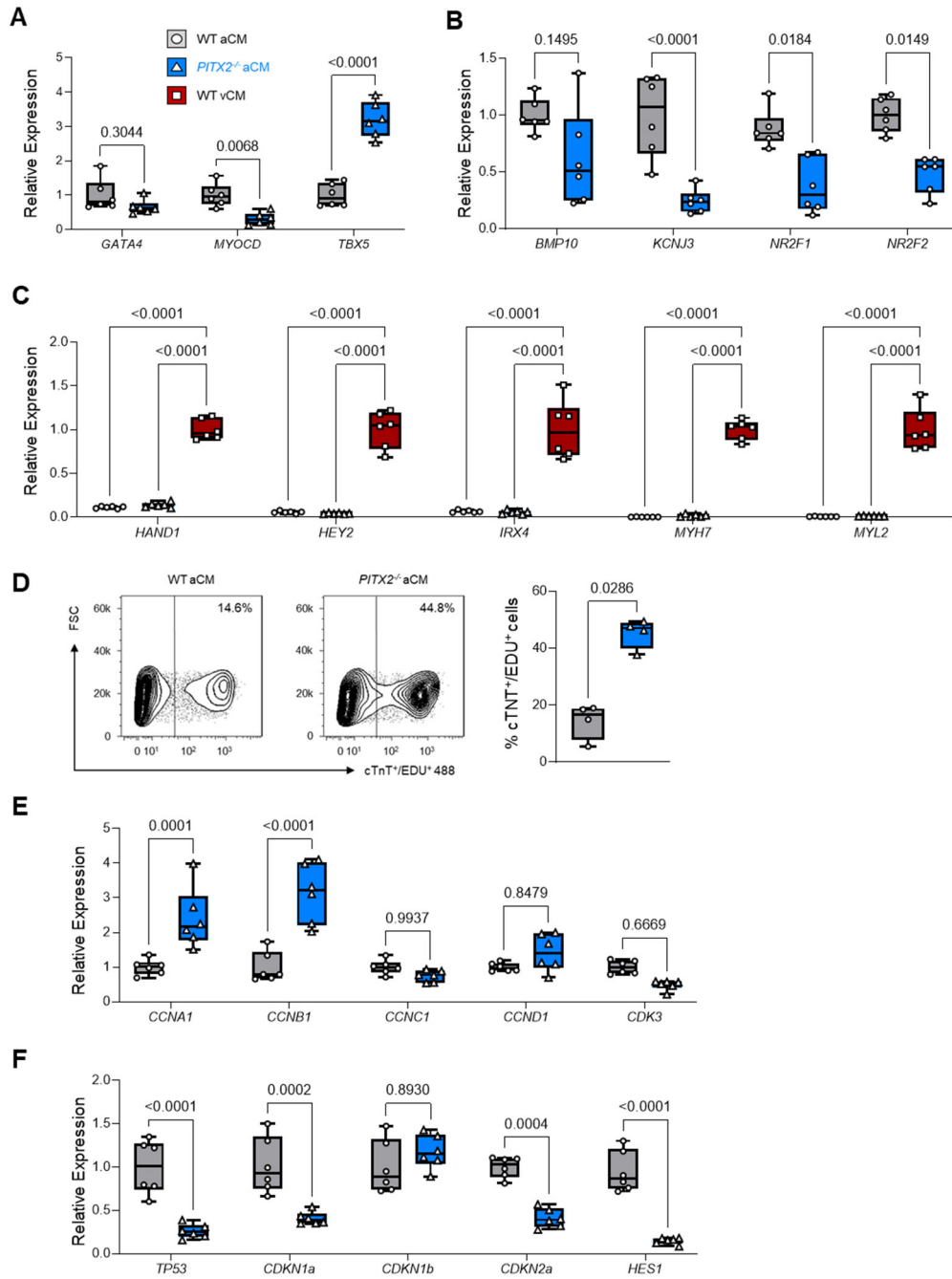
cluster similar action potentials together using K means. Clustering between 2 and 10 clusters was performed. K means clustering was repeated 100 times with random starting values, and the solution which minimized within cluster variance chosen. Final clustering results for 2 or 3 clusters were consistent across multiple iterations of the above approach. Furthermore, optimal clustering (as measuring using Davies–Bouldin, Calinski-Harabasz and Silhouette indices) was always found with 2 or 3 clusters for both spontaneous and stimulated action potentials. Hence, cluster analysis was restricted to 2 or 3 clusters.

Supplementary Figures:



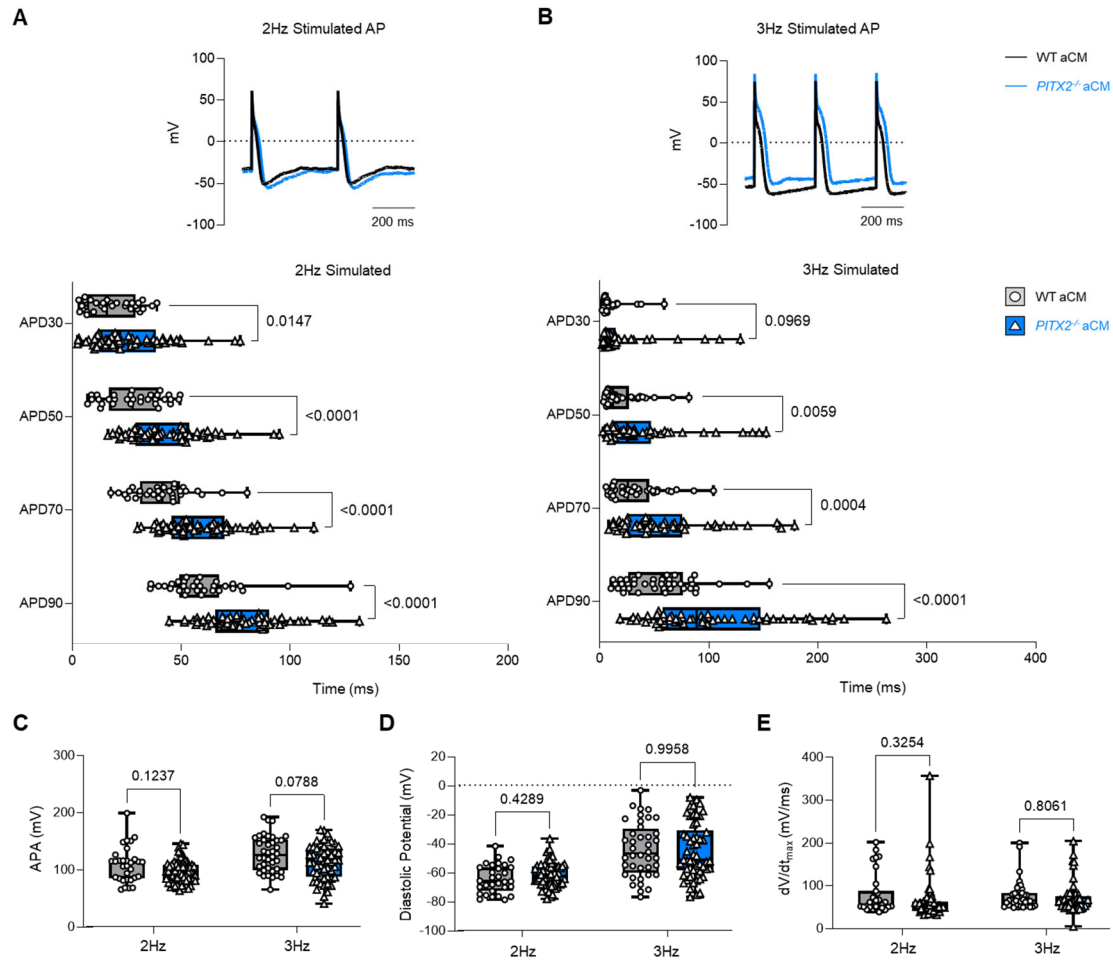
Supplementary Figure 1. Generation of *PITX2*^{-/-} hiPSCs and their differentiation.

(A) Depiction of the deleted at the intron-exon boundary of exon 6 of the *PITX2* gene. Resulting changes in the *PITX2*^{-/-} (KO1 and KO2) hiPSC are marked (arrows). The genetic intervention has been published before (1). (B) Karyotype analysis of WT and *PITX2*^{-/-} hiPSCs using G-banding analysis. (C) Flow cytometry analysis of pluripotency markers OCT4 and SOX2 in WT and *PITX2*^{-/-} hiPSCs. (D) Flow cytometry analysis of Day 12 differentiated atrial cardiomyocytes (aCMs) from WT and *PITX2*^{-/-} lines showing cTnT positive and cTnT/MLC2a double positive cells. Representative flow cytometry plots are shown on the left with quantification on the right (n=6). Data are expressed as the mean relative expression and presented as box and whisker plots (min to max). Statistical analyses were carried out using Mann-Whitney U-tests to compare between two groups.

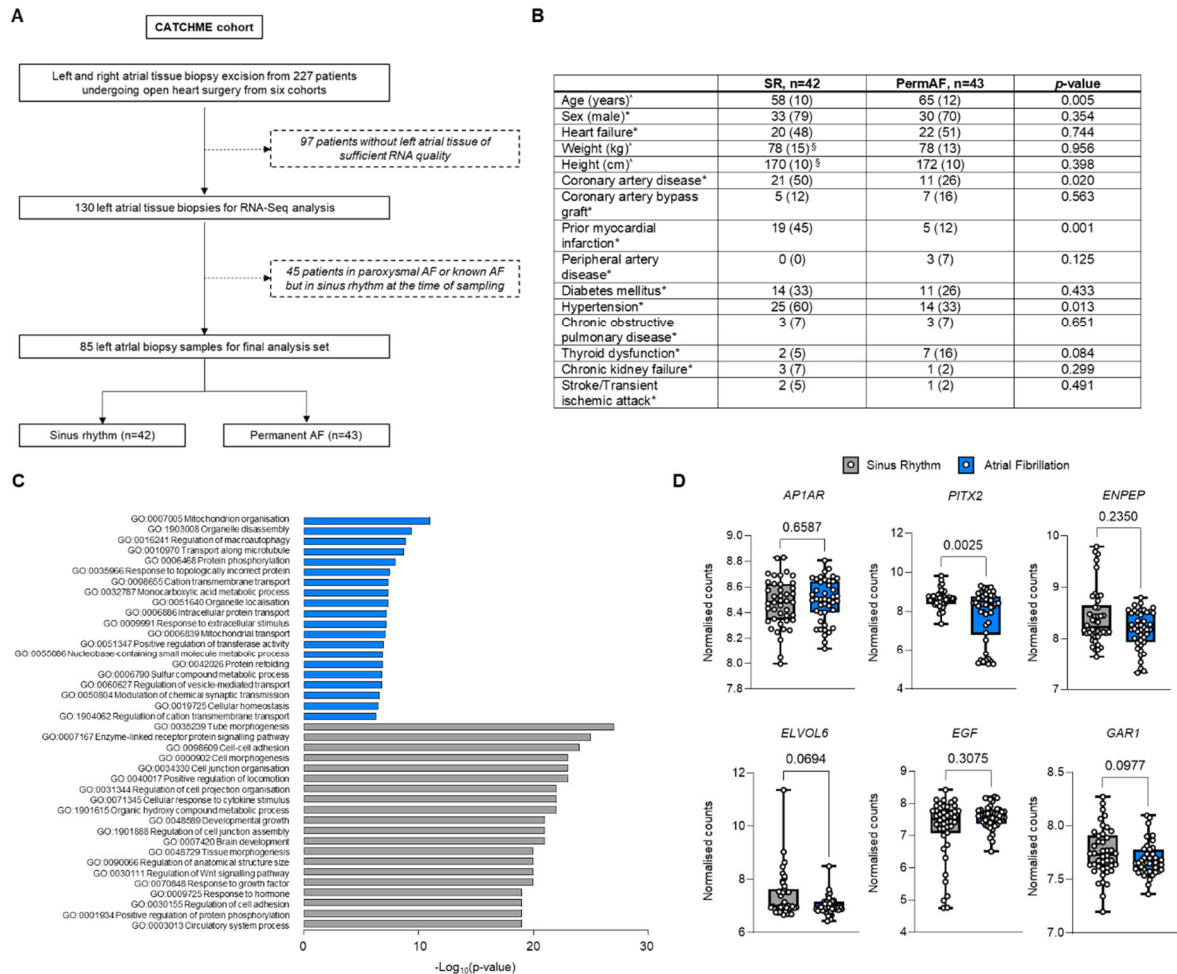


Supplementary Figure 2. Additional characterisation of WT and *PITX2*^{-/-} hiPSC-derived atrial cardiomyocytes (aCMs).

(A) Gene expression of cardiomyocyte development genes *GATA4*, *MYOCD* and *TBX5* in Day 30 WT and *PITX2*^{-/-} aCMs as assessed by RT-qPCR (n=6). (B) Gene expression of atrial cardiomyocyte genes *BMP10*, *KCNJ3*, *NR2F1* and *NR2F2* in Day 30 WT and *PITX2*^{-/-} aCMs as assessed by RT-qPCR (n=6). (C) Gene expression of ventricular cardiomyocyte genes *HAND1*, *HEY2*, *IRX4*, *MYH7* and *MYL2* in day 30 WT aCMs and ventricular cardiomyocytes (vCMs) and *PITX2*^{-/-} aCMs as assessed by RT-qPCR (n=6). (D) Flow cytometry analysis of EDU incorporation in WT and *PITX2*^{-/-} aCMs. Representative flow cytometry plots shown on left with quantification on right (n=4). (E) Gene expression of *CCNA1*, *CCNB1*, *CCNC1*, *CCND1* and *CDK3* in WT and *PITX2*^{-/-} aCMs as assessed by RT-qPCR (n=6). (F) Gene expression of *TP53*, *CDKN1a*, *CDKN1b*, *CDKN2a* and *HES1* in WT and *PITX2*^{-/-} aCMs as assessed by RT-qPCR (n=6). Data are expressed as the mean relative expression and presented as box and whisker plots (min to max). Statistical analyses were carried out using Mann-Whitney U-tests to compare between two groups.

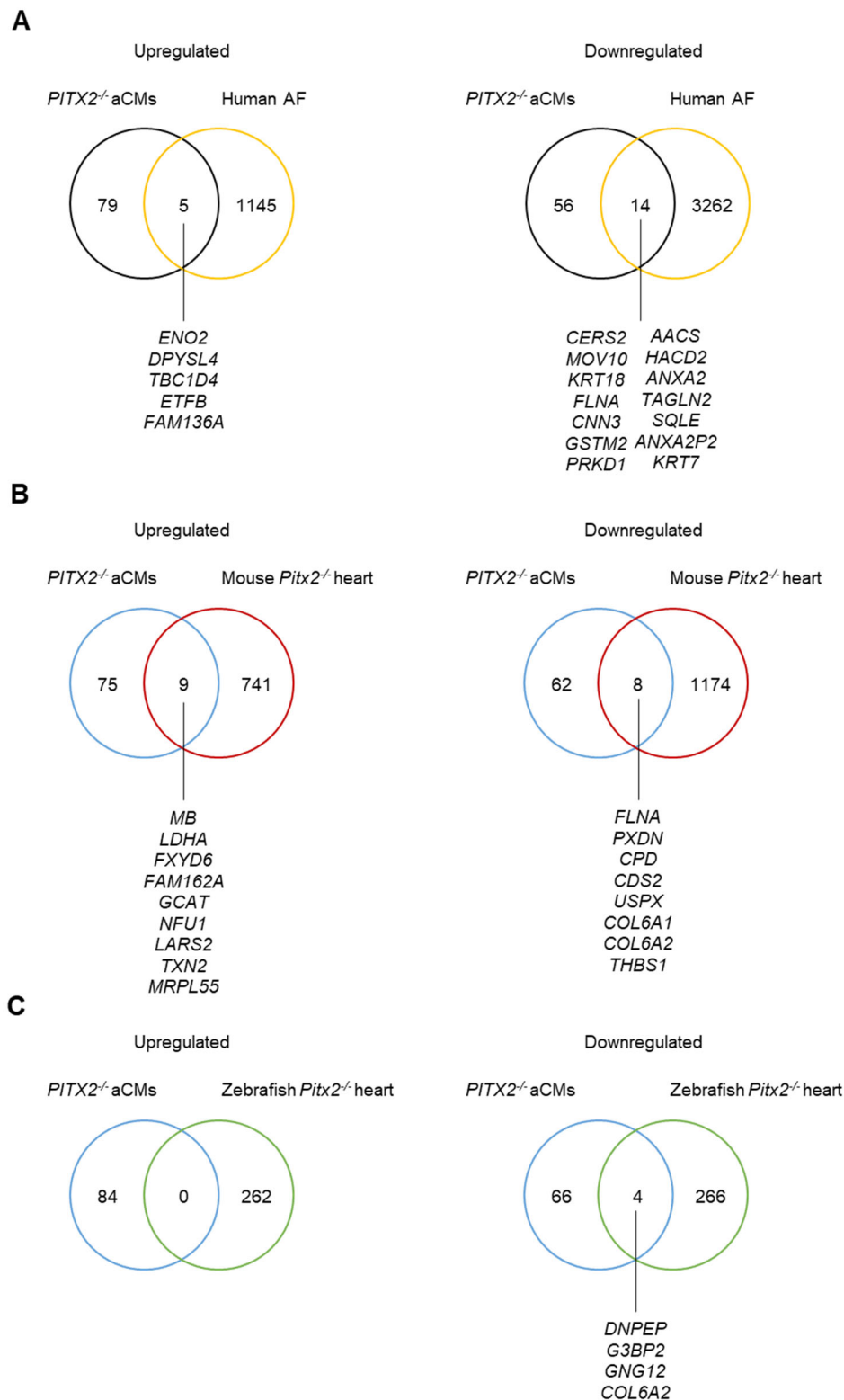


Supplementary Figure 3. Action potential amplitude, diastolic potential and upstroke velocity in WT and *PITX2*^{-/-} aCMs. Representative action potential (AP) traces of 2 Hz (A) or 3 Hz (B) paced WT aCMs and *PITX2*^{-/-} aCMs using whole-cell patch clamp (top). Quantification of action potential duration (APD) at APD30, 50, 70 and 90 in 2 Hz and 3 Hz paced WT and *PITX2*^{-/-} aCMs (2Hz – WT n=31, *PITX2*^{-/-} n=64; 3 Hz WT n=40, *PITX2*^{-/-} n=54 over 5 batches of independently differentiated cells: below). (C) Action potential amplitude (APA), (D) diastolic potential and (E) upstroke velocity (dV/dt_{max}) in 2 Hz and 3 Hz paced WT or *PITX2*^{-/-} aCMs (2Hz – WT n=31, *PITX2*^{-/-} n=64; 3 Hz – WT n=40, *PITX2*^{-/-} n=54). Data are expressed as absolute values and presented as box and whisker plots (min to max). Statistical analyses were carried out using repeated measures ANOVA's to compare between two groups.



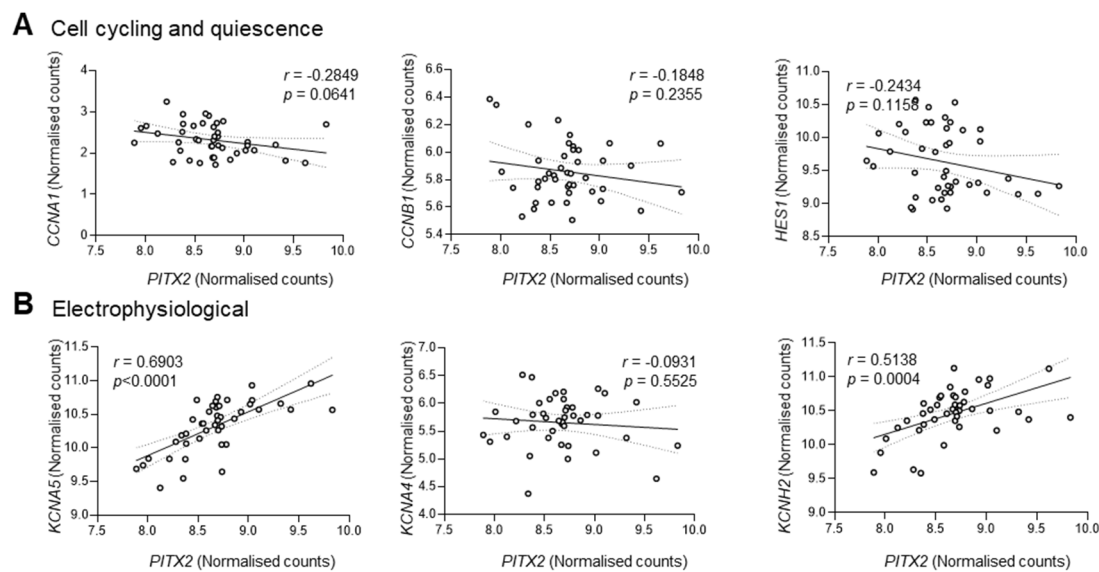
Supplementary Figure 4. Bulk RNA-sequencing of human left atrial appendage tissue.

Left atrial tissue was collected during open heart surgery from patients in sinus rhythm (SR) during the operation ("Sinus Rhythm") and from patients with permanent atrial fibrillation (AF) during surgery. (A) STROBE analysis workflow of left atrial tissue samples. (B) Data are shown as \bar{x} (standard deviation) for continuous variables, or *count (percentage) for dichotomous variables. Differences were tested with independent *t*-test for continuous variables and χ^2 tests or Fisher's exact test (where observations are <5) for dichotomous variables. [§] n=41 due to missing data. SR: patients without a history of AF; AF: persistent or permanent AF, patient in AF at time of tissue sampling. (C) GO biological process analysis highlighting pathways enriched in AF (blue) and in sinus rhythm (grey) patients. (D) Normalised read counts of genes localised around the 4q25 topological associating domain in SR and AF patients (SR n=42; AF n=43). Data are expressed as normalised read counts from DESeq2 analysis and presented as box and whisker plots (min to max). Statistical analyses were carried out using Mann-Whitney U-tests to compare between two groups.

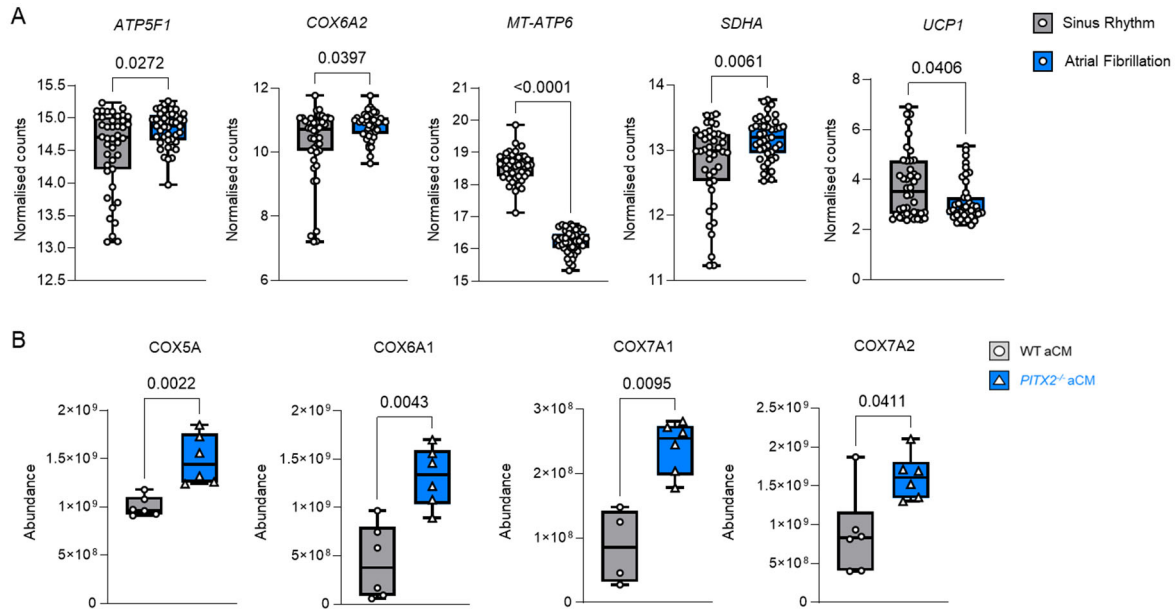


Supplementary Figure 5. Replication of differential expression of genes in *PITX2*^{-/-} aCMs compared to human atrial tissue and *PITX2*-deficient model organisms.

(A) Expression of key differentially expressed genes in sinus rhythm and permanent AF patients (Sinus rhythm n=42; Permanent AF n=43) identified by RNA-Seq compared to proteomic analysis of WT and *PITX2*^{-/-} aCMs; (B) Differentially expressed genes in *Wt* and *Pitx2*^{-/-} mice atrial RNA-Seq compared to proteomic analysis of WT and *PITX2*^{-/-} aCMs; (C) Differentially expressed genes in *Wt* and *Pitx2*^{-/-} zebrafish atrial RNA-Seq compared to proteomic analysis of WT and *PITX2*^{-/-} aCMs.



Supplementary Figure 6. Correlation analysis of *PITX2*-regulated genes in left atrial appendages of patients with chronic (permanent) atrial fibrillation. Correlation analysis of genes implicated in (A) cell cycling and quiescence (*CCNA1*, *CCNB1* and *HES1*), and (B) electrophysiology (*KCNA5*, *KCNA4* and *KCNH2*) with *PITX2*. Data represents $n=43$ with Spearman r values and corrected p -values shown on graphs.



Supplementary Figure 7. Replication of differential expression of mitochondrial genes in human atrial tissue and *PITX2*-deficient aCMs.

(A) Expression of key differentially expressed genes in sinus rhythm (SR) and permanent atrial fibrillation (AF) patients (Sinus rhythm n=42; Atrial Fibrillation n=43). (B) Expression of key differentially-expressed proteins in WT and *PITX2*^{-/-} aCMs (n=6). Data are expressed as the mean relative expression and presented as box and whisker plots (min to max). Data was analysed using a Mann-Whitney U-tests comparing between two groups.

- 1 **Supplementary Table 1.** Antibodies and dilutions used for immunofluorescence, flow cytometry
- 2 and western blot analyses.

Primary antibody	Dilution	Supplier
α -actinin, monoclonal mouse IgG1	1:1,000	Sigma-Aldrich, clone EA-53
cTnT, monoclonal mouse IgG1	1:200	Thermo Fisher Scientific, clone 13-11
GAPDH, monoclonal rabbit IgG	1:10,000	Cell Signalling Technology, clone D16H11
hERG, polyclonal rabbit IgG	1:500	Thermo Fisher Scientific
KCNA5, polyclonal rabbit IgG	1:500	Proteintech
Kir2.2, polyclonal rabbit IgG	1:500	Proteintech
Kv1.4, polyclonal rabbit IgG	1:500	Proteintech
MLC2A, monoclonal mouse IgG2a	1:200	Synaptic Systems, clone 56F5
Nav1.5, monoclonal rabbit IgG	1:500	Cell Signalling Technology, clone D9J7S
OCT3/4, monoclonal IgG2b	1:200	R&D Systems, clone 240408
SOX2, monoclonal mouse IgG2a	1:200	R&D Systems, clone 245610
Secondary antibody	Dilution	Supplier
Alexa Fluor 488, polyclonal goat anti-Rat IgG	1:200	Thermo Fisher Scientific, catalogue A11006
Alexa Fluor 488, polyclonal goat anti-Rabbit IgG	1:200	Thermo Fisher Scientific, catalogue A32731
Alexa Fluor 647, polyclonal goat anti-Mouse IgG	1:200	Thermo Fisher Scientific, catalogue A32728

3

4 **Supplementary Table 2.** Sequences of primers used for qRT-PCR experiments.

Gene	Primer direction	Primer (5' – 3')	Length (bps)	Annealing temperature (°C)
ACTN2	FWD	CTG CTG CTT TGG TGT CAG AG	20	56.2
	REV	TTC CTA TGG GGT CAT CCT TG	20	53.9
ADIPOR2	FWD	GTC TCT CGG CTC TTC TCT AAA C	22	54.5
	REV	CAG CAT CAA CCA GCC TAT CT	20	54.6
BMP10	FWD	GAG AAA GGG AGA AAG GGA AGA G	22	54.7
	REV	CCA GGT AGA GGG AAA TGG TTA G	22	54.5
CACNA1C	FWD	GAG GAA GAG GAG AAG GAG AGA A	22	55.0
	REV	CAG GTC CAG GAT GTT GAA GTA G	22	54.9
CCNA1	FWD	CTC CTC TCC CAG TCT GAA GAT A	22	54.9
	REV	GGA AGT TGA CAG CCA GAT ACA	21	54.5
CCNB1	FWD	CCA GAA CCT GAG CCT GTT AAA	21	54.8
	REV	CTC GAC ATC AAC CTC TCC AAT C	22	55.1
CCNC1	FWD	GGG ACC TAC AGA CAG ACA TAC A	22	55.5
	REV	CAG TAC AGT CCC ACT GAC ATA AC	23	54.9
CCND1	FWD	CAC ACA CAC ACA CAC AAA CC	20	54.8
	REV	CCT CCC TTC AAC ACT TCC TAA A	22	54.4
CD36	FWD	TCT TGG GCA GCA AGT TCT ATA C	22	54.7
	REV	GGA GCA TCT GTG CCT CTA TTT	21	54.7
CDK3	FWD	TCT TGG GCA GCA AGT TCT ATA C	22	54.7
	REV	GGA GCA TCT GTG CCT CTA TTT	21	54.7
CDKN1A	FWD	GGA AGG GAC ACA CAA GAA GAA	21	54.7
	REV	TCC TTG TTC CGC TGC TAA TC	20	55.0
CDKN1B	FWD	GTC AAA CGT GCG AGT GTC TA	20	55.0
	REV	TGC AGG TCG CTT CCT TAT TC	20	55.0
CDKN2A	FWD	TCC TCC CTT CCT TCT CTT ACT C	22	55.1
	REV	GCT TCT GCC TTC CTC TCT AAT C	22	55.0
COX7C	FWD	CCC TTC CTT GTA GTA AGA CAC C	22	54.6
	REV	AAA TCC TGA CCT GGG AAT CAA	21	53.9
FOXO1	FWD	TGG GCA GGA AAG TGA TGT ATA G	22	54.3
	REV	GCA GAA GGG AGA ATG AGA TGA A	22	54.5
GAPDH	FWD	GAT TCC ACC CAT GGC AAA TTC	21	54.6
	REV	GTC ATG AGT CCT TCC ACG ATA C	22	54.8
GATA4	FWD	CTG GCA GTT CCT CTC CTT TAT C	22	54.9
	REV	CCT CCT AAA GTG CTG GGA TTA C	22	55.0
HAND1	FWD	AAT CCT CTT CTC GAC TGG GC	20	56.6
	REV	TGA ACT CAA GAA GGC GGA TG	20	55.0
HES1	FWD	TCA ACA CGA CAC CGG ATA AAC	21	55.1
	REV	GCC GCG AGC TAT CTT TAT TCA	21	57.4
HEY2	FWD	GAT TCA GCC CTC CGA ATG	18	53.1
	REV	TGG CAG AGA GGG ACA AGA	19	56.3
HCN2	FWD	CCG TGG ACT ACA TCT TCC TTA TC	23	54.5
	REV	CAT CTC CTT GTT GCC CTT AGT	21	54.6
HCN4	FWD	GCA CTG GTT TCG CAC TTT AC	20	54.7
	REV	CTA AGC CCA GAC AAT CCC TTA C	22	55.0
IRX4	FWD	TTC CGT TCT GAA GCG TGG TC	20	57.6
	REV	TGA AGC AGG CAA TTA TTG GTG T	22	55.2
KCNA4	FWD	GTC CGT CCT GGT CAT CTT AAT C	22	54.9
	REV	CAG CGA ACC ACAAAC TCA AAG	21	54.7
KCNA5	FWD	CGA GGA TGA GGG CTT CAT TA	20	54.1
	REV	CTG AAC TCA GGC AGG CTC TC	20	57.3
KCND3	FWD	GCC TCA GAC TCA GAC CAA ATA A	22	54.4
	REV	CAG GGA CAG ACA AAG GGT AAG	21	55.1

5

KCNH2	FWD	CTT CCT ATG TCT GGT GGA TGT G	22	54.9
	REV	TGT GGG TTC GCT CCT TTA TC	20	54.8
KCNJ2	FWD	CAC AGT GCC GTA GCT CTT ATC	21	55.3
	REV	GGT CAC ATG GAG ACA TGG TTA G	22	55.2
KCNJ3	FWD	AAAAAC GAT GAC CCC AAA GA	20	52.4
	REV	TGT CGT CAT CCT AGA AGG CA	20	55.4
KCNJ4	FWD	CTT CTG GTG TAT CGC CTT CTT	21	54.5
	REV	CAC CTT GTA GTG GCT CTT CTC	21	55.0
KCNJ5	FWD	TGG ACT CAG AGA GGA GAC TTA C	22	54.9
	REV	CCG ATT CTC CAA TAG GCT ACA C	22	55.0
KCNJ8	FWD	GGA GGA TGA TGA CAG AGG AAT G	22	54.8
	REV	GTG TGG TGA TGC CAG TAG TT	20	55.0
KCNJ11	FWD	CTT CCT GAG TAG CTG GGA TTA C	22	54.5
	REV	CTG GCC TCA CTT CTG AGA TAA C	22	54.9
KCNJ12	FWD	CTT GAT TCT CCT GCC CTC TTT	21	54.7
	REV	GTC TCA TCG CCT ACG TCT TTA G	22	54.8
KCNK3	FWD	AGG TGC CCT CTG TGT TTA TG	20	54.8
	REV	GCG AGT CAG CTA GGT ATG TTA TT	23	54.3
KCNK5	FWD	CAT CAA GCA GAT CGG GAA GAA	21	54.9
	REV	GCT GAG GAT GAT GGA AGG TTA G	22	55.0
KCNK9	FWD	GAG CAG GCC AAA GGG AAA TA	20	55.2
	REV	TAG GTC AGA GAC ACC ACT AAG G	22	55.2
KCNN2	FWD	GGA GCA GAT GAC TGG AGA ATA G	22	54.5
	REV	GAG TAC AGT TCC TGG GCA TAT AG	23	54.4
KCNN3	FWD	GGA ACC TTG TGG GTA AGG TAA G	22	55.1
	REV	GGC CCA GTG CTA CAG AAT AAA	21	54.9
KCNQ1	FWD	CTG TCT TTG CCA TCT CCT TCT	21	54.6
	REV	GCG TCA CCT TGT CTT CTA CTC	21	55.1
LPIN1	FWD	CAG GCT GCT AAG TCT TCT TCT C	22	55.1
	REV	GGT CTC CAG GTC TTC TTC ATT C	22	54.9
MCU	FWD	TCA GTT CAC ACT CAA GCC TAT C	22	54.3
	REV	CCT TCT TCC CTC AGA TCC TTT	22	54.7
MYH6	FWD	CAC CAA CAA TCC CTA CGA CTA C	22	55.0
	REV	CAC TCA ATG CCC TCC TTC TT	20	54.8
MYH7	FWD	CTG TCC TGC TCT GTG TCT TT	20	54.6
	REV	GTA GCG ATC CTT GAG GTT GTA G	22	54.8
MYL2	FWD	GAT GTT CGC CGC CTT CCC CGC	21	66.0
	REV	GCA GCG AGC CCC CTC CTA GT	20	64.1
MYOCD	FWD	TCG ATT TCC AGG GAA GCT AAT C	22	54.5
	REV	CCA CGA GAG GTA ATC AGG AAT G	22	54.9
ND1	FWD	CCC TAA AAC CCG CCA CAT CT	20	57.5
	REV	GAG CGA TGG TGA GAG CTA AGG T	22	58.6
NKX2-5	FWD	AAG TGT GCG TGT GCC TTT	18	55.0
	REV	CTC ATT GCA CGC TGC ATA ATC	21	54.7
NPPA	FWD	ACA GGA TTG GAG CCC AGA G	19	56.8
	REV	GGA GCC TCT TGC AGT CTG TC	20	57.8
NR2F1	FWD	AAG CCA TCG TGC TGT TCA C	19	56.0
	REV	GCT CCT CAG GTA CTC CTC CA	20	57.9
NR2F2	FWD	CCG AGT ACA GCT GCC TCA A	19	57.1
	REV	TTT TCC TGC AAG CTT TCC AC	20	54.0
NRF1	FWD	GGA AGG GAA AGG AAG GA AGA A	22	54.7
	REV	GGT TAC CAA GAA CAC CCA GAT AG	23	55.0
PFKM	FWD	GTG GTT AAG CGT CTG GGA TAT G	22	55.4
	REV	GTT GGA GAC TGT AGC AGG ATT G	22	55.3

PITX2	FWD	CCA GTC TCA ACA GCC TGA ATA A	22	54.6
	REV	TCA TTG CAT CCA CCA GAG AAA	21	54.4
PPARA	FWD	TGA TGT ACC CTG TGC CAT TC	20	54.8
	REV	ATG CCT GAT TTC CTT CCC TAT C	22	54.4
PPARGC1A	FWD	GTG CTA CCT GAG AGA GAC TTT G	22	54.8
	REV	CTC CAT CAT CCC GCA GAT TTA	21	54.5
PRDX5	FWD	GTG GCC TGT CTG AGT GTT AAT	21	54.8
	REV	CTT CAC TAT GCC ATC CTG TAC C	22	55.0
PYGM	FWD	CGG CTG AAG CAG GAG TAT TT	20	55.0
	REV	GGT GAT GCC GTT GGT CTT AT	20	55.1
SCN5A	FWD	TCT TCA CAG GCG AGT GTA TTG	21	54.7
	REV	CAC GAT GAG GAA GGA GAT GAT G	22	54.9
SHOX2	FWD	CCT CCT CCT CCT CTT CTT ACT T	22	55.1
	REV	CCT CCT TCT TCT CCT TCA CTT TC	23	54.9
SLC2A1	FWD	GAT GGG AGT GAG ACA GAA GTA AG	23	54.4
	REV	GTG GGT GGA GTT AAT GGA GTA G	22	54.7
SLC27A1	FWD	GCC ACT ACC TGC CCT TAA AT	20	54.9
	REV	CTG AGG TTC CAG TTT CTC AGT C	22	55.0
SLC27A6	FWD	CTG GTG ACT GTG CTG GAT AAA	21	54.8
	REV	CCA GGA TAG CTG CTG AAC TAT G	22	55.0
SOD1	FWD	GTG CAG GGC ATC ATC AAT TTC	21	54.8
	REV	GCG TTT CCT GTC TTT GTA CTT TC	23	54.4
SOD2	FWD	GGG ATG CCT TTC TAG TCC TAT TC	23	54.7
	REV	CAC CCG ATC TCG ACT GAT TTA C	22	55.1
TBX3	FWD	GAG ATG TTC TGG GCT GGA TAA A	22	54.5
	REV	CTT TGA GGT TCG ATG TCC CTA C	22	55.1
TBX5	FWD	CTC CCT GGC ATC CTA TCT TAT TC	23	54.5
	REV	CCT CAC ATC TTA CCC TGT TCT C	22	54.6
TNNI1	FWD	CTT TAG GGC GTG GGT CTT ATC	21	55.1
	REV	GTA TGC GTG TCC TGG TTA CTT	21	54.7
TNNI3	FWD	TCC AAC TAC CGC GCT TAT G	19	54.9
	REV	TGC CTC TAT GTC GTA TCT CTC T	22	54.4
TNNT2	FWD	GAC ATA GAA GAG GTG GTG GAA G	22	54.6
	REV	CCT CCT CTT TCT TCC TGT TCT C	22	54.6
TP53	FWD	AGT CTA CCT CCC GCC CTC AA	20	55.3
	REV	CCC AAA CAT CCC TCA CAG TAA A	22	54.9

8 **Supplementary Table 3. Patient characteristics stratified by rhythm status.**

Rhythm	Sinus Rhythm, n=42	Atrial Fibrillation, n=43	p-value
Age (years)^	58 (10)	65 (12)	0.005
Sex (male)*	33 (79)	30 (70)	0.354
Heart failure*	20 (48)	22 (51)	0.744
Weight (kg)^	78 (15) §	78 (13)	0.956
Height (cm)^	170 (10) §	172 (10)	0.398
Antiarrhythmic drugs (Amiodarone, flecainide, dronedaron, propafenone, sotalol)*	1 (2)	8 (19)	0.016
Coronary artery disease*	21 (50)	11 (26)	0.020
Prior myocardial infarction*	19 (45)	5 (12)	0.001
Coronary artery bypass graft*	5 (12)	7 (16)	0.563
Peripheral artery disease*	0 (0)	3 (7)	0.125
Diabetes mellitus*	14 (33)	11 (26)	0.433
Hypertension*	25 (60)	14 (33)	0.013
Chronic obstructive pulmonary disease*	3 (7)	3 (7)	0.651
Thyroid dysfunction*	2 (5)	7 (16)	0.084
Chronic kidney failure*	3 (7)	1 (2)	0.299
Stroke/Transient ischemic attack*	2 (5)	1 (2)	0.491

9 Left atrial tissue was collected during open heart surgery from patients without known atrial
10 fibrillation and in sinus rhythm during the operation (“Sinus Rhythm”) and from patients with
11 permanent atrial fibrillation including during surgery. Data are shown as ^mean (standard deviation)
12 for continuous variables, or *count (percentage) for dichotomous variables. Differences were tested
13 with independent t-test for continuous variables and X² tests or Fisher’s exact test (where
14 observations are <5) for dichotomous variables. Sinus Rhythm: patients without a history of AF; Atrial
15 Fibrillation: persistent/permanent AF.

Supplementary Table 4. Analysis of nuclear parameters in WT aCMs and *PITX2*^{-/-} aCMs.

Values are given as mean ± SEM. A total of 63 images of WT aCMs and 62 images from *PITX2*^{-/-} aCMs over three experiments were analysed using a nested ANOVA. *P*-values are denoted.

Parameter	WT aCM	<i>PITX2</i> ^{-/-} aCM	<i>P</i> value
Number per field	10.53 ± 6.49	21.63 ± 10.75	<0.0001
Area (µm ²)	76.30 ± 40.34	132 ± 37.33	<0.0001
Perimeter (µm)	30.17 ± 8.51	41.47 ± 5.93	<0.0001
Feret's diameter (µm)	10.09 ± 2.95	13.53 ± 2	<0.0001
Length (µm)	11.12 ± 1.98	10.79 ± 2.34	0.5786
Width (µm)	5.46 ± 1.13	5.52 ± 1	0.7368
Eccentricity	0.65 ± 0.03	0.56 ± 0.06	<0.0001
Solidity	0.96 ± 0.02	0.93 ± 0.02	<0.0001

Supplementary Table 5. Proteomics data of *PITX2*^{-/-} aCMs compared to WT aCMs. n = 6 *PITX2*^{-/-} aCMs and n = 6 WT aCMs independent differentiation experiments at day 30.

1515 proteins with log2 fold < 0, of which 68 were significantly higher expressed in WT aCMs				1613 proteins with log2 fold < 0, of which 82 were significantly higher expressed in <i>PITX2</i> ^{-/-} aCMs			
Protein ID	Protein Name	<i>PITX2</i> ^{-/-} aCM Vs WT aCM ratio	Significance (p.adj)	Protein ID	Protein Name	<i>PITX2</i> ^{-/-} aCM Vs WT aCM ratio	Significance (p.adj)
P07996	Thrombospondin-1	-4.18	0.00917	P02144	Myoglobin	3.41	0.0405
P08729	Keratin, type II cytoskeletal 7	-3.55	0.0317	P00338	L-lactate dehydrogenase A chain	3.41	0.0463
Q86WU2	Probable D-lactate dehydrogenase, mitochondrial	-3.22	0.019	P21397	Amine oxidase [flavin-containing] A	3.3	0.024
P12110	Collagen alpha-2(VI) chain	-3.13	0.0232	Q9HoQ3	FXFD domain-containing ion transport regulator 6	3.21	0.00507
P51911	Calponin-1	-3.1	0.00917	P61812	Transforming growth factor beta-2 proprotein	3.21	0.024
Q96C86	m7GpppX diphosphatase	-2.66	0.0232	Q4VC31	Protein MIX23	2.95	0.0348
P40938	Replication factor C subunit 3	-2.49	0.0374	Q96A26	Protein FAM162A	2.79	0.0348
Q9Y5Q8	General transcription factor 3C polypeptide 5	-2.43	0.0232	P58107	Epiplakin	2.77	0.0296
Q13642	Four and a half LIM domains protein 1	-2.41	0.0284	O75600	2-amino-3-ketobutyrate coenzyme A ligase, mitochondrial	2.69	0.0291
P13497	Bone morphogenetic protein 1	-2.21	0.024	Q6JQN1	Acyl-CoA dehydrogenase family member 10	2.64	0.018
Q96SQ9	Cytochrome P450 2S1	-2.18	0.0232	P09104	Gamma-enolase	2.6	0.0499
P50281	Matrix metalloproteinase-14	-2.14	0.0315	Q9UMS0	NFU1 iron-sulfur cluster scaffold homolog, mitochondrial	2.53	0.018
P23921	Ribonucleoside-diphosphate reductase large subunit	-2.11	0.0159	P54578	Ubiquitin carboxyl-terminal hydrolase 14	2.52	0.018
Q9Y371	Endophilin-B1	-2.09	0.022	Q13740	CD166 antigen	2.49	0.0454
A6NMY6	Putative annexin A2-like protein	-2.05	0.024	Q7Z4H8	Protein O-glucosyltransferase 3	2.39	0.024
P29536	Leiomodin-1	-1.99	0.0243	P13637	Sodium/potassium-transporting ATPase subunit alpha-3	2.28	0.0452
P12109	Collagen alpha-1(VI) chain	-1.98	0.0232	P35241	Radixin	2.18	0.0271
Q9BQ67	Glutamate-rich WD repeat-containing protein 1	-1.97	0.0288	Q13049	E3 ubiquitin-protein ligase TRIM32	2.17	0.0479
Q14534	Squalene monooxygenase	-1.93	0.0399	Q8WWV3	Reticulon-4-interacting protein 1, mitochondrial	2.1	0.0291
Q15050	Ribosome biogenesis regulatory protein homolog	-1.89	0.024	O15212	Prefoldin subunit 6	2.09	0.0479
P37802	Transgelin-2	-1.88	0.022	P36871	Phosphoglucosmutase-1	2.05	0.0348
Q9GZM7	Tubulointerstitial nephritis antigen-like	-1.87	0.0269	P30405	Peptidyl-prolyl cis-trans isomerase F, mitochondrial	2.03	0.024
P24347	Stromelysin-3	-1.86	0.00917	Q9HCC0	Methylcrotonoyl-CoA carboxylase beta chain, mitochondrial	2.02	0.0239

P07355	Annexin A2	-1.83	0.0293	Q9NPL8	Complex I assembly factor TIMMDC1, mitochondrial	2.01	0.0479
Q13509	Tubulin beta-3 chain	-1.79	0.00917	O15020	Spectrin beta chain, non-erythrocytic 2	2	0.0499
Q6Y1H2	Very-long-chain (3R)-3-hydroxyacyl-CoA dehydratase 2	-1.79	0.0159	P51159	Ras-related protein Rab-27A	1.94	0.0499
Q9BPX3	Condensin complex subunit 3	-1.76	0.0445	Q6PI78	Transmembrane protein 65	1.89	0.0487
O95084	Serine protease 23	-1.76	0.0495	P22392	Nucleoside diphosphate kinase B	1.87	0.044
Q99996	A-kinase anchor protein 9	-1.74	0.0178	P11166	Solute carrier family 2, facilitated glucose transporter member 1	1.86	0.0292
P35251	Replication factor C subunit 1	-1.74	0.018	Q96CN7	Isochorismatase domain-containing protein 1	1.82	0.0499
P10589	COUP transcription factor 1	-1.72	0.0396	P09429	High mobility group protein B1	1.78	0.0466
P24468	COUP transcription factor 2	-1.72	0.0396	Q92743	Serine protease HTRA1	1.76	0.00249
Q93008	Probable ubiquitin carboxyl-terminal hydrolase FAF-X	-1.64	0.0416	Q9UJC5	SH3 domain-binding glutamic acid-rich-like protein 2	1.75	0.0454
Q14966	Zinc finger protein 638	-1.63	0.0254	Q9HAV7	GrpE protein homolog 1, mitochondrial	1.73	0.0288
Q5T160	Probable arginine--tRNA ligase, mitochondrial	-1.6	0.024	Q16595	Frataxin, mitochondrial	1.7	0.044
Q9UBG0	C-type mannose receptor 2	-1.59	0.0232	Q969S9	Ribosome-releasing factor 2, mitochondrial	1.69	0.0254
P21266	Glutathione S-transferase Mu 3	-1.57	0.0177	B2RPK0	Putative high mobility group protein B1-like 1	1.63	0.0293
O95674	Phosphatidate cytidyltransferase 2	-1.54	0.0414	Q643R3	Lysophospholipid acyltransferase LPCAT4	1.58	0.0293
Q99584	Protein S100-A13	-1.48	0.0338	Q9H078	Caseinolytic peptidase B protein homolog	1.56	0.024
Q86V21	Acetoacetyl-CoA synthetase	-1.46	0.0305	P41247	Patatin-like phospholipase domain-containing protein 4	1.55	0.0466
P37268	Squalene synthase	-1.46	0.0315	Q9BXX5	Bcl-2-like protein 13	1.55	0.0499
Q14257	Reticulocalbin-2	-1.45	0.0243	Q5TZA2	Rootletin	1.54	0.0384
Q66K79	Carboxypeptidase Z	-1.44	0.0479	Q8N490	Probable hydrolase PNKD	1.52	0.0311
Q9UBI6	Guanine nucleotide-binding protein G(I)/G(S)/G(O) subunit gamma-12	-1.42	0.0269	P05026	Sodium/potassium-transporting ATPase subunit beta-1	1.47	0.0291
Q8IZ52	Chondroitin sulfate synthase 2	-1.42	0.0269	O14531	Dihydropyrimidinase-related protein 4	1.44	0.0178
O75976	Carboxypeptidase D	-1.38	0.0483	P61604	10 kDa heat shock protein, mitochondrial	1.44	0.0292
O60831	PRA1 family protein 2	-1.36	0.0382	P15531	Nucleoside diphosphate kinase A	1.42	0.0288
O75475	PC4 and SFRS1-interacting protein	-1.31	0.0431	O75380	NADH dehydrogenase [ubiquinone] iron-sulfur protein 6, mitochondrial	1.42	0.037
P17655	Calpain-2 catalytic subunit	-1.3	0.0338	Q96ER9	Mitochondrial potassium channel	1.41	0.0452
O75352	Mannose-P-dolichol utilization defect 1 protein	-1.3	0.0348	P80404	4-aminobutyrate aminotransferase, mitochondrial	1.38	0.024

Q9UN86	Ras GTPase-activating protein-binding protein 2	-1.29	0.0499	P10599	Thioredoxin	1.38	0.0454
Q15139	Serine/threonine-protein kinase D1	-1.28	0.018	Q96DA6	Mitochondrial import inner membrane translocase subunit TIM14	1.35	0.0293
O00139	Kinesin-like protein KIF2A	-1.26	0.019	Q99747	Gamma-soluble NSF attachment protein	1.34	0.0293
Q15417	Calponin-3	-1.26	0.0232	Q9Y2J2	Band 4.1-like protein 3	1.34	0.0431
P28161	Glutathione S-transferase Mu 2	-1.26	0.0414	Q9BZF1	Oxysterol-binding protein-related protein 8	1.3	0.0291
Q9HD20	Endoplasmic reticulum transmembrane helix translocase	-1.23	0.0284	O00409	Forkhead box protein N3	1.26	0.0284
Q9P2K5	Myelin expression factor 2	-1.22	0.0293	Q9NX40	OCIA domain-containing protein 1	1.26	0.0499
P18085	ADP-ribosylation factor 4	-1.22	0.0454	Q15031	Probable leucine--tRNA ligase, mitochondrial	1.25	0.0269
Q9ULA0	Aspartyl aminopeptidase	-1.21	0.0293	O60343	TBC1 domain family member 4	1.23	0.0232
P21333	Filamin-A	-1.2	0.018	Q9BYT8	Neurolysin, mitochondrial	1.23	0.0291
Q92626	Peroxidasin homolog	-1.2	0.024	P0CB38	Polyadenylate-binding protein 4-like	1.23	0.0479
Q14195	Dihydropyrimidinase-related protein 3	-1.19	0.0232	Q96RQ3	Methylcrotonoyl-CoA carboxylase subunit alpha, mitochondrial	1.22	0.0269
P05783	Keratin, type I cytoskeletal 18	-1.16	0.044	P05165	Propionyl-CoA carboxylase alpha chain, mitochondrial	1.22	0.0291
Q9H3P7	Golgi resident protein GCP60	-1.15	0.0293	Q9PoV9	Septin-10	1.2	0.0291
P52292	Importin subunit alpha-1	-1.14	0.0293	O95319	CUGBP Elav-like family member 2	1.2	0.0479
Q9HCE1	Helicase MOV-10	-1.12	0.0479	O60313	Dynamin-like 120 kDa protein, mitochondrial	1.19	0.0422
P06239	Tyrosine-protein kinase Lck	-1.11	0.0292	P42126	Enoyl-CoA delta isomerase 1, mitochondrial	1.17	0.0479
Q96G23	Ceramide synthase 2	-1.09	0.0271	P22307	Sterol carrier protein 2	1.16	0.0159
				Q8N4Q1	Mitochondrial intermembrane space import and assembly protein 40	1.15	0.018
				Q9BXW7	Haloacid dehalogenase-like hydrolase domain-containing 5	1.15	0.018
				P14927	Cytochrome b-c1 complex subunit 7	1.14	0.0374
				Q96RP9	Elongation factor G, mitochondrial	1.09	0.0291
				P19338	Nucleolin	1.09	0.0348
				Q9H3G5	Probable serine carboxypeptidase CPVL	1.07	0.018
				Q9UPT5	Exocyst complex component 7	1.07	0.0473
				P38117	Electron transfer flavoprotein subunit beta	1.06	0.0479
				P00367	Glutamate dehydrogenase 1, mitochondrial	1.05	0.024
				Q96C01	Protein FAM136A	1.04	0.0489

				Q99757	Thioredoxin, mitochondrial	1.04	0.0499
				Q7Z7F7	39S ribosomal protein L55, mitochondrial	1.03	0.0489
				Q9GZT3	SRA stem-loop-interacting RNA-binding protein, mitochondrial	1.02	0.0232
				P49448	Glutamate dehydrogenase 2, mitochondrial	1.01	0.018

Supplementary Table 6. Distribution and characteristics of identified action potential phenotypes. *p<0.05, **p<0.01, ***p<0.001, ****p<0.0001 versus cluster 1. #p<0.05, ##p<0.01, ###p<0.001, ####p<0.0001 versus cluster 2.

Parameter	1 Hz paced			2 Hz paced			3 Hz paced		
	Cluster 1	Cluster 2	Cluster 3	Cluster 1	Cluster 2	Cluster 3	Cluster 1	Cluster 2	Cluster 3
Proportion of all cells (%)	40.2	43.8	16.0	35.5	37.6	26.9	36.6	37.6	25.8
Membrane potential (mV)	-67.2±1.0	-50.4±1.0****	27.9±3.7****###	-57.6±0.9	-60.7±1.5	72.0±0.8****#	-62.5±1.3	40.8±1.6****	25.2±3.6****###
Maximum upstroke velocity (mV/ms)	77.1±5.3	63.3±3.1*	63.2±3.1	52.2±1.6	66.0±9.2	95.2±10.8**#	82.5±7.3	68.9±4.5	63.1±3.9
Action potential amplitude (mV)	113.6±3.6	110.3±3.9	119.9±6.2	93.0±3.7	98.6±3.8	109.1±5.8*	119.2±4.6	114.6±6.3	121.8±6.2
APD30 (ms)	22.0±1.8	17.9±1.8	17.4±6.2	14.7±1.3	31.4±3.3****	23.3±2.5	18.3±3.6	9.3±2.0	17.0±6.2
APD50 (ms)	37.2±2.2	33.2±2.5	35.3±9.5	26.9±1.7	50.7±3.2****	36.2±2.6*###	37.4±4.9	19.7±3.3	33.3±9.3
APD70 (ms)	51.0±2.3	51.9±3.1	59.6±12.9	40.7±1.7	67.8±2.9***	48.9±2.8####	55.1±5.7	38.6±4.9	50.4±10.9
APD90 (ms)	68.3±2.7	82.0±4.1	102.7±16.0**	61.2±2.2	90.9±2.7***	66.6±3.9####	78.6±7.0	84.7±10.4	91.3±13.2
Proportion of WT aCMs (%)	50.0	36.6	13.4	46.7	6.7	46.7	38.5	38.5	23.1
Proportion of <i>PITX2</i> ^{-/-} aCMs (%)	33.0	49.1	17.9	30.2	52.4	17.5	35.2	37.0	27.8

28 **Supplementary Table 7. Gene set enrichment analysis of enriched pathways from genes significantly upregulated in the left atria of**
 29 **patients in permanent AF.**

GO	Description	Count	%	-Log ₁₀ (p-value)	Genes
GO:0007005	mitochondrion organization	45	5.97	14.74	<i>SLC25A5,BAK1,BNIP3,CALM3,COX7A2,MARK2,HSPA4,HSP90AA1,HSPD1,MPV17,NDUFA10,SPG7,ULK1,HIP1R,LONP1,MTRF1,ATG13,MFN2,COX17,TIMM17A,TIMM44,WDR45,TRAK1,ATG4B,PMPCA,GABARAPL1,SNX7,ARMCX3,TTC19,WIPI1,SLC25A36,ATAD3A,FOXRED1,AGK,MTRF1L,ATPAF1,FUNDC2,TRAK2,CHCHD7,MAP1LC3B,RHOT2,COX19,NDUFA11,IMMP1L,MPV17L</i>
GO:0031329	regulation of cellular catabolic process	56	7.43	12.09	<i>SLC25A5,ATP6V1B2,ATP6V1C1,ATP6VoB,ATP6VoA1,BNIP3,MAPK14,DAPK3,MTOR,GOLGA2,HSF1,DNAJB2,MLH1,CDK16,PGAM1,PRKAA2,SGTA,TSC1,UCHL1,VDAC1,BAG6,TFEB,EPM2A,RBM10,ULK1,MAPKAPK2,BAG3,ATP6V1G1,RNF14,FEZ2,ATG13,OPTN,ARIH2,ZER1,HAX1,IGF2BP2,WDR45,EXOSC7,SAMD4A,MTCL1,MLYCD,MKRN2,CCDC22,PACSIN3,SNX7,ZCCHC17,TENT5C,ALKBH5,WIPI1,FBXW7,TRIM39,FYCO1,VPS26B,CCNY,STING1,SH3RF3,HSP90AA1,PRKCE</i>
GO:1903008	organelle disassembly	19	2.52	11.00	<i>BNIP3,MARK2,GOLGA2,KIF5B,PRKAA2,ULK1,GBF1,ATG13,WDR45,ATG4B,GABARAPL1,SNX7,UFC1,WIPI1,KIF9,FUNDC2,UBA5,MAP1LC3B,STING1,ARSB,CALM1,CTSD,MTOR,HSP90AA1,TFEB,BAG3,TECPR2,MFN2,OPTN,ARL8B,ACBD5,UBXN2A,PAM5,TMEM41B,ATP6VoB,ATP6VoA1,ATP6AP1,SYT7,LAPTM4B,EPHA4,HMGA1,HSPA2,MICAL2,EXOGBMERB1,HSF1,PRKAG1,TSC1,VDAC1,MITF,RHOT2,NPAS2,FYCO1</i>
GO:0006886	intracellular protein transport	47	6.23	9.20	<i>ARF1,ATP6AP1,HSPA4,HSP90AA1,HSPD1,KIF5B,sort1,SEC13,SGTA,SSR3,BAG6,RAB28,BAG3,ZFYVE16,TECPR2,MFN2,PREB,TIMM17A,TIMM44,YWHAQ,VPS45,COPZ1,COPG1,TRAK1,GGA2,PMPCA,ICMT,SEC61G,SEC31B,ARL5A,ZDHHC2,STX18,AKIRIN2,AGK,KIF13A,C17orf75,TRAK2,ASPSCR1,MLPH,GRIP2,COG3,COG7,TMEM129,VPS26B,IMMP1L,TMED4,RILPL1,BICD1,CALM3,PRKAA2,RAD21,SKP1,GBF1,SUPT7L,DNAJB6,OPTN,DCTN2,SUN1,POT1,TERF2IP,PACS1,OBSCN,TAPT1,LEMD2,EMC10,MPV17,VDAC1,GNPAT,COX17,MLYCD,CHCHD7,COX19,ACBD5</i>
GO:0035966	response to topologically incorrect protein	20	2.65	9.12	<i>BAK1,CCND1,COMP,HSF1,DNAJB2,HSPA2,HSPA4,HSP90AA1,HSPD1,BAG6,BAG3,MFN2,OPTN,HSPH1,DNAJB4,HSPA14,AKIRIN2,NGLY1,KBTBD6,TMEM129,MTOR,SEC13,MAPKAPK2,DNAJB6,CHORDC1,CCT6A,CCT4,HSP90AA2P,DNAJA4</i>
GO:0006468	protein phosphorylation	47	6.23	8.92	<i>ACVR2B,BAK1,CCND1,MAPK14,DAPK3,DMPK,MARK2,EPHA4,MTOR,GAS6,GRK4,MARK1,MAP3K10,CDK16,PDCK3,PDPK1,PKM,PPP3CB,PRKAA2,PRKAG1,PRKAR1B,PRKCE,PTPN4,RAF1,RPS6KA2,ST3GAL1,ULK1,RIOK3,DYRK1B,MAPKAPK2,ATG13,TNK2,STK38,AAK1,CILK1,MAST2,TAOK3,CAB39,MAP3K20,TRPM7,ALPK3,MARK4,RPS6KL1,OBSCN,BSRK1,NEK7,TTBK2,EOGT</i>
GO:0010657	muscle cell apoptotic process	8	1.06	8.80	<i>BNIP3,DMPK,HSP90AA1,RPS6KA2,RBM10,BAG3,KIFAP3,MYOCD,HSF1,PDPK1,MFN2</i>

GO:0032787	monocarboxylic acid metabolic process	38	5.04	8.74	ACADVL,ACAT1,ASAH1,CPT2,MAPK14,DBI,ENO2,ETFB,ETFDH,GPI,HAGH,LDHB,PGAM1,PGK1,PKM,PRKAA2,PRKAG1,SLC6A8,TPI1,VDAC1,GNPAT,PLA2G4C,CES2,QKI,DHRS9,SLC27A4,MLYCD,PLA2G15,ACOT11,OXSM,GBA2,PTGES2,MCEE,ACBD5,HOGA1,PTGR3,GATD1,SLC27A1,ARF1,ARSB,SLC25A20,ESRRA,INPP4A,INPPL1,NPAS2,OXCT1,PCYT1A,ABCB4,RXRB,SMPD1,MTMR1,HDAC3,MAPKAPK2,PPT2,STAR10,NEU3,ACOT9,TIAM2,PI4K2A,AGK,STARD7,PLEKHA2,TBL1XR1,PTDSS2,LCLAT1,INPP5A,ST3GAL4,DGKZ,DGKD,DGKI,BCAT2,UPP1,ENTPD4,ACAD8,PAFAH2,PLCE1,PLCXD3
GO:0010970	transport along microtubule	19	2.52	7.62	BICD1,KIF5B,SPG7,UCHL1,BAG3,COPG1,CILK1,TRAK1,KIFAP3,KIF1B,SUN1,ARMCX3,ARL8B,KIF13A,TRAK2,FYCO1,RHOT2,IFT43,TMEM201,MFN2,MARK2,MARK1,KIFC3,DNAAF5,KIF9,KLC2,KLC4
GO:0006839	mitochondrial transport	18	2.39	7.36	SLC25A5,BAK1,BNIP3,SLC25A20,CPT2,HSPA4,HSP90AA1,HSPD1,SPG7,HIP1R,MFN2,TIMM17A,TIMM44,PMPCA,AGK,RHOT2,IMMP1L,MPV17L,CALM3,MTOR,LAPTM4B,VDAC1,HAX1,FBXW7,PGAM5
GO:0051640	organelle localization	35	4.64	7.06	BICD1,CALM1,MARK2,MTOR,KIF5B,MARK1,MLH1,UCHL1,TFEB,GBF1,MFN2,PREB,DCTN2,YKT6,BVES,COPG1,TRAK1,KIFAP3,PLEKHM2,SUN1,FAM98A,TRAPPC3,ARMCX3,TRAPPC2L,DEF8,WIPI1,ARL8B,KIF13A,C17orf75,KLC2,TRAK2,MLPH,FYCO1,RHOT2,TMEM201
GO:0010498	proteasomal protein catabolic process	29	3.85	6.99	DNAJB2,PSMD13,SGTA,SKP1,UCHL1,RNF103,BAG6,BTRC,SOCS6,AREL1,MAEA,PSME4,NEDD4L,FBXO9,ANAPC7,FBXW5,RNF216,AKIRIN2,ANKZF1,FBXW7,NGLY1,RMND5A,TBL1XR1,FBXO31,DDI2,ZNRF1,KBTD6,TMEM129,UBXN2A,ARF1,CALM1,CALM2,CALM3,CTSD,MTOR,ITGAV,KIF5B,PDPK1,PPP2CA,PPP3CB,RAF1,SEC13,THOP1,TPP2,RNF14,ACTR1B,ARIH2,DCTN2,RAPGEF4,KIFAP3,SEC61G,MKRN1,ASB1,BTBD1,TRIM39,UBE2O,KLC2,UBA5,KLC4,BNIP3,HSP90AA1,LONP1,BAG3,ZER1,USP20,ADAMTS7,USP47,USP46,MKRN2,DCAF15,FEN1,MLH1,SMG7,EXOG,EXOSC7,SAMD4A,SMG5,RAB40B,RNF141,KLHL24,CCNB1IP1,ARRDC4,LNX2,SH3RF3,UF C1
GO:0055086	nucleobase-containing small molecule metabolic process	38	5.04	6.91	ACAT1,ADCY6,ATP6V1B2,CTNS,ENO2,MTOR,GLRX,GPI,LDHB,NDUFA10,PDE7A,PGAM1,PGK1,PKM,SDHA,TPI1,UPP1,PUDP,PDE8B,MBD4,PPT2,ENTPD4,VPS9D1,ATP5MG,NT5C2,NMNAT2,MLYCD,ICMT,ACOT9,ACOT11,OXSM,NMNAT1,MCEE,NDUFA11,OARD1,NEIL2,ATP5F1EP2,MTHFD2L,ACADVL,COX7A2,ETFB,ETFDH,GIPR,GSR,GYG1,OXCT1,PPP1R3C,MTFR1,COX17,SIRT3,GABARAPL1,MTFR1L,COQ9,CIAPIN1,INPP4A,INPPL1,PCYT1A,GNPAT,DGKZ,DGKD,PLA2G4C,MTMR1,SOCS6,EFR3B,PI4K2A,PTDSS2,LCLAT1,SLC27A1
GO:0010638	positive regulation of organelle organization	34	4.51	6.60	SLC25A5,BAK1,BNIP3,CCT6A,CD47,FEN1,MTOR,PRKCE,RAD21,TSC1,VDAC1,ULK1,HIP1R,MCRS1,HAX1,CCT4,NES,WDR45,PNKP,SYNPO,POT1,SH2B1,SNX7,ANAPC7,STX18,TERF2IP,WIPI1,ARHGEF10L,MARK4,FYCO1,ATF7IP2,NEK7,PGAM5,TAPT1,HSF1,HSP90AA1,FAM98A,PLCE1,DEF8,FNIP1

GO:0051668	localization within membrane	35	4.64	6.39	ATP6AP1,CALM3,DLG3,GAS6,GOLGA4,HSPA4,HSP90AA1,LRP4,SGTA,SSR3,BAG6,COLQ,OPTN,MYL12A,RAB40B,EFR3B,GGA2,NFASC,ICMT,SEC61G,GORASP2,ARL5A,CCDC22,EHD3,ZDHHC2,SNX7,CCDC93,VPS53,PACS1,AGK,KIF13A,GRIP2,ZFYVE27,EMC10,RILPL1,SORT1,GBF1,WIP1
GO:0051347	positive regulation of transferase activity	36	4.77	6.06	ACVR2B,CCND1,CALM1,CALM2,CALM3,DBI,DLG3,DOCK3,MARK2,EPHA4,FGF1,M TOR,GAS6,HSP90AA1,MAP3K10,PDPK1,PPP2CA,PRKAG1,SKP1,DGKZ,BTRC,UNC119,DAZAP2,CIB1,CCT4,AKAP13,PNKP,POT1,TAOK3,CAB39,FBXW7,ALS2,ARRDC4,NEK7,CCNY,SLC27A1,DUSP3,PRKAR1A,PRKAR1B,SMPD1,TSC1,UCHL1,DIRAS3,STK38,CHORDC1,PLCE1,SH3BP5L,MYOCD,SOCS6,HSF1,HSPA2,LRP4,RAF1,HDAC3,TNK2,HAX1,NPTN,SLCO3A1,TERF2IP,FNIP1

30

31 **Supplementary Table 8. Gene set enrichment analysis of enriched pathways from genes significantly downregulated in the left atria of**
 32 **patients in permanent AF.**

GO	Description	Count	%	-Log ₁₀ (p-value)	Genes
GO:0150076	neuroinflammatory response	4	1.90	3.77	<i>ADCY8,CNTF,IFNG,TRPV1,GRIA1,GRM8,SLC1A2,PCSK1</i>
GO:0015800	acidic amino acid transport	4	1.90	3.68	<i>SLC1A2,SLC3A1,SLC6A13,TRPV1,SLC6A20,SLC8A3,SLC22A7,RHCG</i>
GO:0098655	cation transmembrane transport	14	6.67	3.35	<i>CACNA1B,KCNQ3,P2RX5,SLC1A2,SLC6A13,SLC8A3,TRPV1,KCNQ4,RHCG,SLC6A20,TMEM163,CATSPER1,UNC80,LRRC52,SYNGR3,GABRA6</i>
GO:0006836	neurotransmitter transport	6	2.86	3.41	<i>SLC1A2,SLC6A13,SYNGR3,CPLX1,ERC2,SYT2,TACR2,CACNA1B</i>
GO:0002377	immunoglobulin production	6	2.86	3.08	<i>IGKV1D-33,IGKV3-15,IGKV2-24,IGKV1-39,IGKV1-17,IGKV1-6</i>
GO:0033198	response to ATP	3	1.43	2.85	<i>P2RX5,P2RY2,TRPV1,GABRA6,GRIA1</i>
GO:0043269	regulation of ion transport	12	5.71	2.33	<i>CACNA1B,IFNG,KCNQ3,P2RX5,TACR2,FGF23,KCNQ4,CATSPER1,JSRP1,SYT2,MIR208A,LRRC52,ADCY8</i>
GO:0065004	protein-DNA complex assembly	6	2.86	2.27	<i>CENPA,H3C6,H4C8,MED17,TAF7L,TSPYL6</i>
GO:0060632	regulation of microtubule-based movement	3	1.43	2.17	<i>TACR2,CALY,CATSPER1</i>
GO:0006873	cellular ion homeostasis	8	3.81	2.02	<i>ADCY8,GDF2,GRIA1,P2RY2,SLC8A3,FGF23,RHCG,VPS33A</i>

33

34 **Supplementary References:**

- 35 1. Marczenke M, Fell J, Piccini I, Ropke A, Seebohm G, and Greber B. Generation and cardiac subtype-
36 specific differentiation of PITX2-deficient human iPS cell lines for exploring familial atrial fibrillation.
37 *Stem cell research*. 2017;21:26-8.
- 38 2. Zhang X, Smits AH, van Tilburg GB, Ovaa H, Huber W, and Vermeulen M. Proteome-wide
39 identification of ubiquitin interactions using UbIA-MS. *Nat Protoc*. 2018;13(3):530-50.
- 40 3. Yu G, Wang LG, Han Y, and He QY. clusterProfiler: an R package for comparing biological themes
41 among gene clusters. *OMICS*. 2012;16(5):284-7.
- 42 4. Ng AY, Jordan MI, and Weiss Y. On Spectral Clustering: Analysis and an Algorithm. *Adv Neural Inf*
43 *Process Syst*. 2001:849-56.
- 44 5. Gorospe G, Zhu R, Millrod MA, Zambidis ET, Tung L, and Vidal R. Automated grouping of action
45 potentials of human embryonic stem cell-derived cardiomyocytes. *IEEE Trans Biomed Eng*.
46 2014;61(9):2389-95.